

Original Research

Lithology and Human Activities Determine the Distribution and Pollution Level of Potentially Toxic Elements in the Topsoil of the Karst Region, Southwestern China

Chunlai Zhang^{1,2}, Weijie Li¹, Tongbin Zhu¹, Xia Zou^{1,3*}, Ling He⁴

¹Key Laboratory of Karst Dynamics, Ministry of Natural Resources and Guangxi, Institute of Karst Geology, Chinese Academy of Geological Sciences, Guilin 541004, PR China

²School of Environmental Studies, China University of Geosciences, Wuhan 430078, PR China

³School of Medical Laboratory, Guilin Medical University, Guilin 541004, PR China

⁴Institute of Geophysical and Geochemical Exploration, Chinese Academy of Geological Sciences, Langfang 065000, PR China

Received: 30 December 2021

Accepted: 25 May 2022

Abstract

Potentially toxic elements (PTE) pollution in soils has become a major global environmental problem, and their spatial distribution and risk assessment are essential issues of concern to human beings. To analyze the distribution characteristics and the pollution levels of arsenic, cadmium (Cd), chromium, copper, mercury, nickel, lead and zinc in soil, 573 surface soil samples were collected from the karst region (karst area, K; denudation monadnock with solutional cap rock, KSC; non-karst area, NK) in Mashan County, Guangxi Province. The pollution load index (PLI), potentially ecological risk index (RI) and Nemerow composite pollution index (NCPI) were employed to assess the pollution levels of PTE. The PLI and RI results revealed that the soils have undergone relatively low-moderate contamination due to the high geological background. The average concentration of PTE in different soils were in the following decreasing order, K>KSC>NK. The concentration of Cd in 75.74% of samples exceeded the risk screening values of GB 15618-2018. The relatively high pollution level of PTE was mainly distributed in K soil, rich in calcium, magnesium and an alkaline environment. Therefore, there is a higher risk of pollution in areas with high background of heavy metals in karst areas. The clean-precaution and light pollution levels in the NCPI risk assessment were distributed in NK and KSC areas, respectively. However, metal ores and human activities caused the deviation of the clean-low risk and lithological distribution in the NK and KSC areas. The adjacent

NK and KSC should also pay attention to the dangers of heavy metal pollution caused by mining and human activities.

Keywords: potentially toxic elements, surface soil, risk assessment, karst region, human activities, lithology, spatial distribution

Introduction

Heavy metal pollution in geoponic soils is an acute environmental concern owing to its toxicological effects on biological and ecological systems [1-3]. Once heavy metals enter plants, and animals, most of them will accumulate there for a long time, resulting in various complications. For example, heavy metals can damage the roots, leaves, cell components and other organs of plants, and even interfere with critical biochemical processes, such as photosynthesis and minerals absorption [4]. Also, they can damage the essential organs of the animals' bodies, such as the kidney and liver, even causing cancer [4]. Plants on soil contaminated by heavy metals threaten the health of animals and people who eat meat from grazing animals [5]. Although there are many influencing factors for heavy metals to enter the body of residents through diets, such as pH and the bioavailability of the elements in soil, the total amount of elements is still the first factor to be considered. Scientists from Asia, Europe, America and other regions have been increasingly concerned about the source apportionment of heavy metals in soil [6].

Around one-fifth of farmland has been reported to be contaminated with potentially toxic elements (PTE) in China [7]. High concentrations of Cd and Pb were found in south, southwest, and northwest China [8]. Eight provinces in southwest China have approximately 0.51 million km² of exposed carbonate rock areas, accounting for 5.8% of the total land [9]. The karst area is one of the main areas with a high geological setting of PTE. Due to the secondary enrichment of PTE during the process of carbonate weathering and pedogenesis, the resulting soil has a significantly high concentration of PTE [10-11]. The first national pollutant survey reflected that the concentration of arsenic (As), cadmium (Cd), chromium (Cr), copper (Cu), mercury (Hg), nickel (Ni), lead (Pb) and zinc (Zn) in the surface soils of Guangxi were 2.0, 4.5, 1.6, 1.1, 2.6, 1.3, 1.4 and 1.4 times than that of the surface soils of China, respectively. However, part of croplands with high heavy metal geological settings were used to culture crops owing to the finite arable land per capita in China, especially the karst area in Southwest China [12].

Parent material determines the heavy metal content in soil [13]. At present, there is a lot of research on soil heavy metal pollution in karst areas [10, 12-14]. In karst areas, carbonate rocks intercalated with clastic rocks or interbedded between the two are common. They vary in mineral composition, weathering mode and degree. But

comparative studies on PTE between karst areas and non-karst areas are even rarer. The spatial distribution characteristics and risk assessment of the heavy metals of soil in carbonate rocks and non-carbonate rocks, as well as the denudation monadnock with solutional cap rock, are particularly critical. Furthermore, human activities, such as mining, smelting and improper disposal of wastes, expose heavy metals to the surface at a higher rate than natural processes, resulting in high risk of heavy metal pollution [15-16]. Pollution caused by human activities makes the prediction of heavy metals in the soil much more difficult. Therefore, the objectives of this study were 1) to investigate the concentration and distribution of 8 PTE (As, Cd, Cr, Cu, Hg, Ni, Pb and Zn) in soils; 2) to assess the risk of heavy metal pollution in K and NK, and their relationship with lithology and human activities.

Materials and Methods

Study Area

Mashan County is located northwest of Nanning City, Guangxi Province, China (Fig. 1). The annual average precipitation is 1722.5 mm, and the yearly average temperature is 21.8°C in this area [17]. Karst areas are distributed in the western and eastern of Mashan County, which contains thick limestone layers and dolomitic limestone intercalations. Soils developed in the karst area are dominated by brown rendzina. There are mainly shrubs in karst mountainous areas and abandoned cultivated land in depressions. Non-carbonate rocks comprise sandstones and mudstones, which are distributed in the west, south, and central part of the study area, and the land uses include secondary forests and reservoirs. Between the karst and non-karst areas, the denudation monadnock with solutional cap rock (KSC) among clastic mountains had formed owing to the tectogenesis and favourable water catchment conditions. The KSC is surrounded by Quaternary sediments of varying thicknesses, overlying diamicton that is dominated by loamy and clayey sediments, and the land uses include paddy fields, drylands, and construction land.

Samples

The surface soil samples (0-20 cm) were sampled every km² in 2016, covering the main land uses and soil types in the study area. The sampling sites were arranged in the middle of the grid where the terrain is

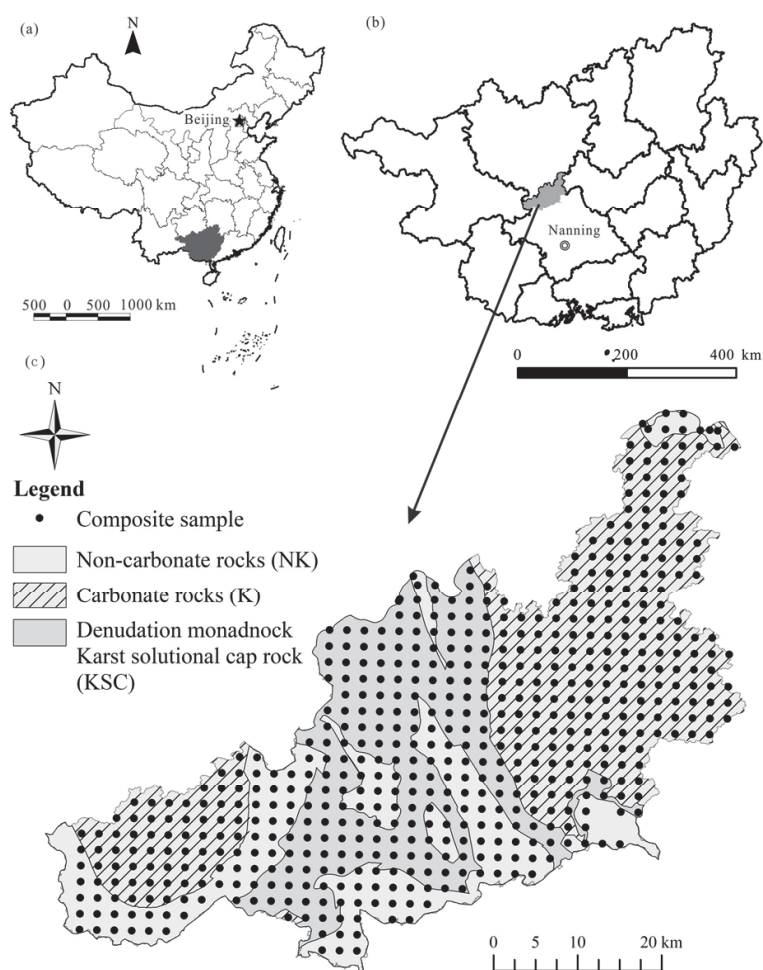


Fig. 1. Map of sampling site and geological background.

flat, and slopes is gentle, or low-lying areas between mountains where the soil is congregated easily from hilly and mountainous karst areas. At each sampling site, three sub-samples were collected within 50 m and combined into one soil sample. When sampling, the litter of ground plants was scraped off, and weeds, roots, gravel, bricks, and other debris were removed. The sample drying and processing site was free from pollution. Samples were lightly tapped with a mallet to their natural size, and gone through a 2 mm nylon sieve. Then, four soil samples of even-numbered kilometre grids were combined into a composite sample for laboratory analysis. A total of 573 composite samples data (K, 321; KSC, 114; NK, 138, respectively) were obtained in this study. Field sampling was carried out under the Specification of multi-purpose regional geochemical survey (DZ/T0258-2014) [18].

Laboratory Analysis

Major elements of soil were measured by an X-ray fluorescence spectrometer (Rigaku Corporation, Japan, ZSX Primus II) using fused glass beads. The concentration of Cd, Cr, Cu, Pb, Ni and Zn were measured using ICP- mass spectrometry (Perkin Elmer

Inc., USA, NexION 300) after digestion of the soil samples with <math><0.074\text{-mm}</math> particle size with an HCl – HF – HClO₄ – HNO₃ mixture. As and Hg was determined by atomic fluorescence spectroscopy after the soil sample was digested with aqua regia, and reduced with Potassium Borohy. The pH values were measured by a PHS-3C pH meter at a ratio of 1:2.5 (soil: CO₂ free water). The soil organic matter (SOM) was determined through titration using the potassium dichromate oxidation–ferrous ammonium sulphate method. And 12 national reference materials such as GBW 07447–GBW 07449, GBW 07451, GBW 07455, and GBW 07385–GBW 07391 were selected to test the accuracy and precision of the analysis. The technical parameters met the “Specifications of the Multi-purpose Regional Geochemical Survey” (DZ/T0258-2014).

PTE Contamination Assessment

Single Pollution Index (P_i)

The Single pollution index (P_i) used to assess heavy metal pollution in the soil is calculated as follows [19]. The P_i values of PTE in soil were calculated by the following formula:

$$P_i = C_i / C_{REF_i} \tag{1}$$

where C_i and C_{REF_i} is the concentration of PTE “i” (mg/kg) in the soil and background value in the study area. Correspondingly, the pollution degree of single element is divided into five levels: clean ($P_i < 1$), low ($1 \leq P_i < 2$), moderate ($2 \leq P_i < 3$), equivalent ($3 \leq P_i < 5$) and extremely high ($P_i > 5$).

Nemeiro Comprehensive Pollution Index

The Nemeiro Comprehensive Pollution Index (NCPI) is commonly used for comprehensive pollution evaluation of heavy metals, and expressed as:

$$NCPI = \sqrt{(P_{i_{max}}^2 + P_{i_{ave}}^2)} / 2 \tag{2}$$

where $P_{i_{max}}$ and $P_{i_{ave}}$ represent the maximum and average P_i value of PTE, respectively. According to NCPI, the pollution degree of PTE is divided into five levels: clean (≤ 0.7), prevention (0.7~1.0), light pollution (1.0~2.0), moderate (2.0~3.0) and heavy pollution (> 3.0) [20].

The pollution load index (PLI) was proposed to represent the total pollution of all PTE in the soil, which was calculated as follows:

$$PLI = \sqrt[n]{P_{i_1} \times P_{i_2} \times \dots \times P_{i_n}} \tag{3}$$

The pollution degree is divided into four levels for a single heavy metal and group-PTE: clean ($PLI \leq 1$), low ($1 < PLI \leq 2$), moderate ($2 < PLI \leq 3$) and high ($PLI > 3$), respectively.

The Potentially Ecological Risk Index (RI)

The potentially ecological factor (PEF) has been widely applied to assess the ecological risk of toxic

PTE in soils [21-22]. The PEF values are calculated as follows:

$$PEF_i = Tr_i \times P_i = Tr_i \times C_i / C_{REF_i} \tag{4}$$

where Tr_i is the biological toxicity coefficient for heavy metal i (10, 30, 2, 5, 40, 5, and 1 for As, Cd, Cr, Cu, Hg, Pb and Zn, respectively) [21-23]. The potentially ecological risk index (RI) can be calculated by the following function:

$$RI = \sum_{i=1}^n PEF_i \tag{5}$$

The contamination degree is further grouped into low ($PEF < 40$, $RI < 90$), moderate ($40 \leq PEF < 80$, $90 < RI \leq 180$), considerable ($80 \leq PEF < 160$, $180 < RI \leq 360$) and high ($PEF > 160$, $RI > 360$), respectively.

Data Analysis

Descriptive statistics and normal distribution tests were performed using PASW statistics 18 (SPSS Inc., Chicago, IL, USA). The spatial distribution maps of PTE in the soil were drawn in ArcGIS 10.2 (Esri, USA). The correlation diagram and boxplots were plotted by RStudio and Origin 8.5 (OriginLab, USA), respectively.

Results and Discussion

Concentration of PTE in Soils and Geochemical Distribution

The statistical analysis of PTE and pH was shown in Table 1. The average concentration of As, Cd, Cr, Cu, Hg, Ni, Pb and Zn in soil were 22.15 ± 13.27 , 2.35 ± 2.52 ,

Table 1. Descriptive analysis of the heavy metal concentration in soil.

Item	As	Cd	Cr	Cu	Hg	Ni	Pb	Zn	pH
Min	3.06	0.05	27	10.81	0.05	0.28	12.7	23.6	4.21
Max	56.3	9.97	380.1	77.78	0.52	176.69	106.4	601.2	8.45
Mean	22.15	2.35	138.65	39.89	0.20	60.43	44.39	197.90	6.14
SD	13.27	2.52	85.06	12.78	0.11	39.73	22.03	144.10	0.98
CV(%)	59.91	107.31	61.35	32.05	55.46	65.76	49.64	72.81	16.00
Skewness	0.54	1.22	1.05	0.22	0.65	0.68	0.40	0.67	0.31
Kurtosis	-0.84	0.53	0.15	-0.33	-0.38	-0.59	-1.18	-0.59	-1.13
Background value	22.15	2.38	140.39	40.13	0.20	60.43	44.43	199.48	6.14
Topsoil of Guangxi	8	0.144	50	18	0.083	15	24	43	/
R	2.77	16.32	2.77	2.23	2.41	4.03	1.85	4.60	/

CV is the coefficient of variation, $CV = 100\% \times SD/mean$; R is the ratio of the background values of this study to Guangxi [24]; elements are in mg/kg, pH is dimensionless.

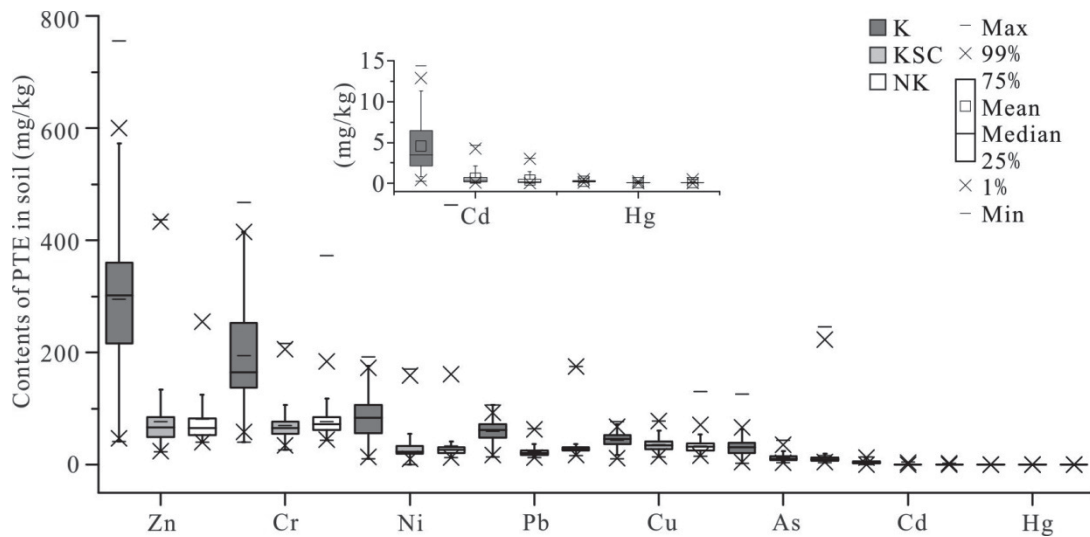


Fig. 2. Boxplots of PTE's concentration in soil in the study area. K, KSC, and NK represent the karst area, denudation monadnock with solutional cap rock, and non-karst area, respectively.

138.65±85.06, 39.89±12.78, 0.2±0.11, 60.43±39.73, 44.39±22.03 and 197.9±144.1 mg/kg, respectively. The soil pH values disclosed strong acid to alkaline status, with values in the range of 4.21-8.45. The ratio of the background values of the study area to that in Guangxi [24] was calculated and recorded as *R* (Table 1). Cd had the highest *R* value of 16.32, followed by Hg, with the *R*-value of 4.60. All PTE in topsoil had higher concentrations than Guangxi, and the lowest Cu and Pb in the study area were also 2.22 and 1.85 times more than that of it. The *R*-value in the study area is

consistent with the percentage of the karst distribution area. Karst covers an area of 1629.35 km² or about 69.48% of Mashan County, which is 1.7 times more than that of Guangxi's 40.9% [25].

The coefficient of variation (CV) of the PTE in the soil followed the sequence of: Cd (107.31%), Zn (72.81%), Ni (65.76%), Cr (61.35%), As (59.91%), Hg (55.46%), Pb (49.64%), and Cu (32.05%), respectively (Table 1), indicating that the concentration of the PTE varied fairly. The CVs of Cd were greater than 100%, showing an extremely variable with uneven distribution.

Table 2. Correlation coefficients of elements and pH in soil.

	As	Cd	Cr	Cu	Hg	Mn	Ni	Pb	Zn	Si	Al	Fe	CaMg	pH
As	1	0.407	0.486	0.473	0.493	0.459	0.498	0.704	0.552	-0.541	0.504	0.568	0.316	0.413
Cd	0.407	1	0.835	0.371	0.700	0.618	0.537	0.635	0.773	-0.533	0.489	0.582	0.263	0.539
Cr	0.486	0.835	1	0.432	0.788	0.542	0.673	0.670	0.807	-0.604	0.564	0.657	0.317	0.585
Cu	0.473	0.371	0.432	1	0.492	0.614	0.744	0.545	0.649	-0.562	0.537	0.608	0.298	0.379
Hg	0.493	0.700	0.788	0.492	1	0.618	0.762	0.710	0.855	-0.653	0.603	0.703	0.382	0.667
Mn	0.459	0.618	0.542	0.614	0.618	1	0.677	0.612	0.664	-0.513	0.445	0.595	0.275	0.500
Ni	0.498	0.537	0.673	0.744	0.762	0.677	1	0.650	0.882	-0.651	0.600	0.693	0.405	0.619
Pb	0.704	0.635	0.670	0.545	0.710	0.612	0.650	1	0.816	-0.847	0.812	0.854	0.478	0.656
Zn	0.552	0.773	0.807	0.649	0.855	0.664	0.882	0.816	1	-0.778	0.728	0.806	0.456	0.711
Si	-0.541	-0.533	-0.604	-0.562	-0.653	-0.513	-0.651	-0.847	-0.778	1	-0.972	-0.965	-0.621	-0.643
Al	0.504	0.489	0.564	0.537	0.603	0.445	0.600	0.812	0.728	-0.972	1	0.954	0.452	0.517
Fe	0.568	0.582	0.657	0.608	0.703	0.595	0.693	0.854	0.806	-0.965	0.954	1	0.478	0.588
CaMg	0.316	0.263	0.317	0.298	0.382	0.275	0.405	0.478	0.456	-0.621	0.452	0.478	1	0.714
pH	0.413	0.539	0.585	0.379	0.667	0.500	0.619	0.656	0.711	-0.643	0.517	0.588	0.714	1

All coefficients are significantly correlated at *p* < 0.01.

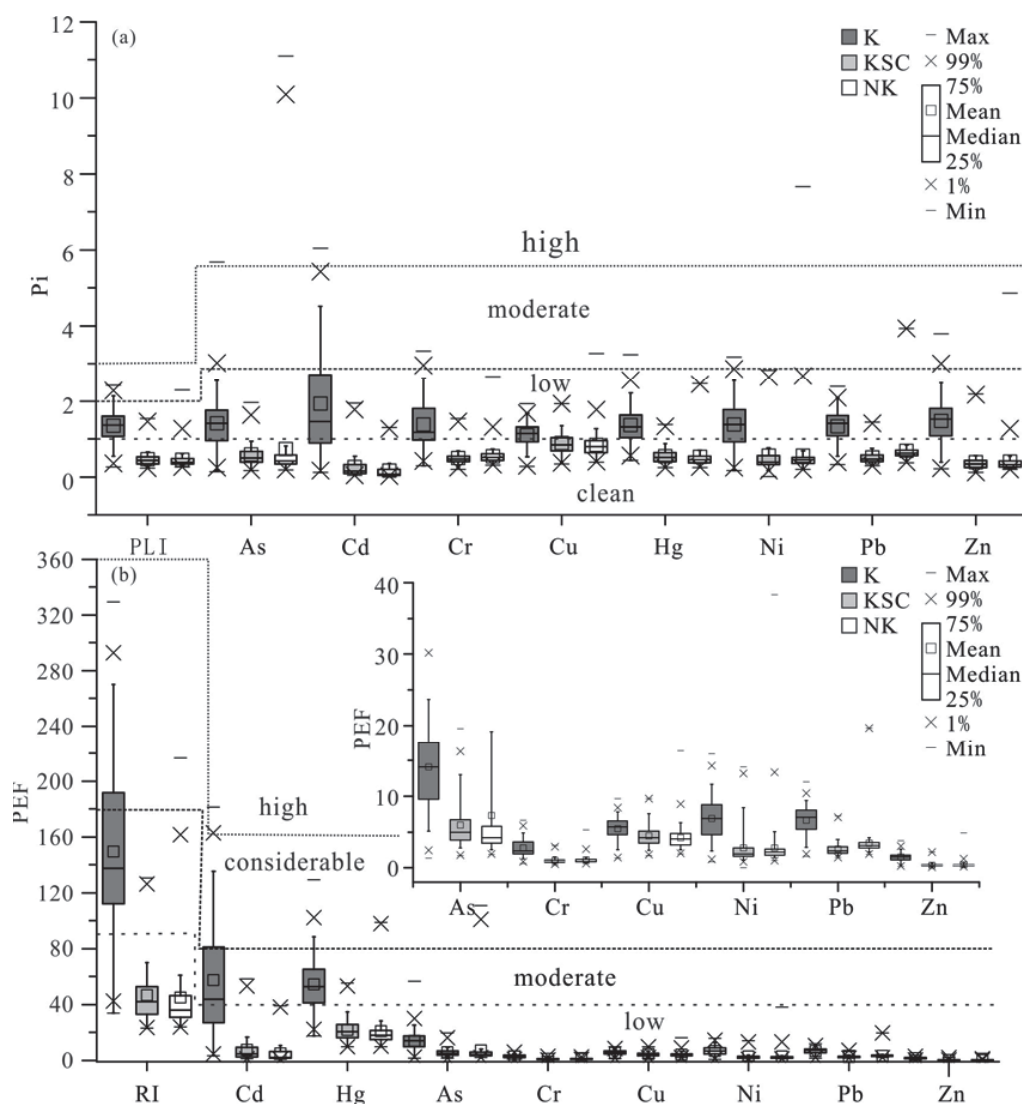


Fig. 3. Contamination and risk assessment of PTE in the soils:

a) pollution load index (PLI) and single pollution index (P_i). The sparse, loose, and dense dotted line distinguish the level of clean, low, moderate, and heavy pollution; b) potentially ecological risk index (RI) and potentially ecological factor (PEF), the dotted line has the same meaning as (a).

In addition, the Kolmogorov-Smirnov normality test results showed that the concentrations of all elements were skewed.

The concentration of PTE in K was higher than that in KSC and NK (Fig. 2). The high concentrations of soil As, Cd, Cr, Cu, Hg, Pb, Zn, TFe_2O_3 , CaO, and pH were distributed in the eastern region and northwest of Mashan, were mainly covered by carbonate rock. The low-value PTE was primarily distributed in the central area and the southern part of Mashan County, where the soil parent material is mainly non-carbonate rock. Cu and Ni showed high background values in the central area, mainly affected by manganese ore.

The pH values in K were higher than NK and KSC. 62.83% of the soil sample in the study area was acid ($5.0 \leq \text{pH} < 6.5$)-strong acid ($\text{pH} < 5.0$). Strong acid soil accounted for 36.82% of the total samples, which were mainly distributed in the NK area, and acid soils were

concentrated in KSC. While neutral ($6.5 \leq \text{pH} < 7.5$) and alkaline ($7.5 \leq \text{pH} < 8.5$) soils accounted for 25.13% and 12.04% of the study area, respectively, and which were mainly distributed in the K area.

Correlation Analysis for Source Identification of PTE in Soil

The correlations between the concentration of metals and pH in soil were demonstrated in Table 2. The concentration of As, Cd, Cr, Cu, Hg, Ni, Pb, Zn, and pH in soils was a significant positive correlation with each other ($p < 0.01$). All the studied PTE were significantly positively correlated with Al, Fe and Mn, suggesting that PTE in soils may be affected by ferromanganese oxide and aluminium-rich clay minerals [26]. The distribution and speciation of PTE in soil and aquatic systems are controlled by Fe-Mn

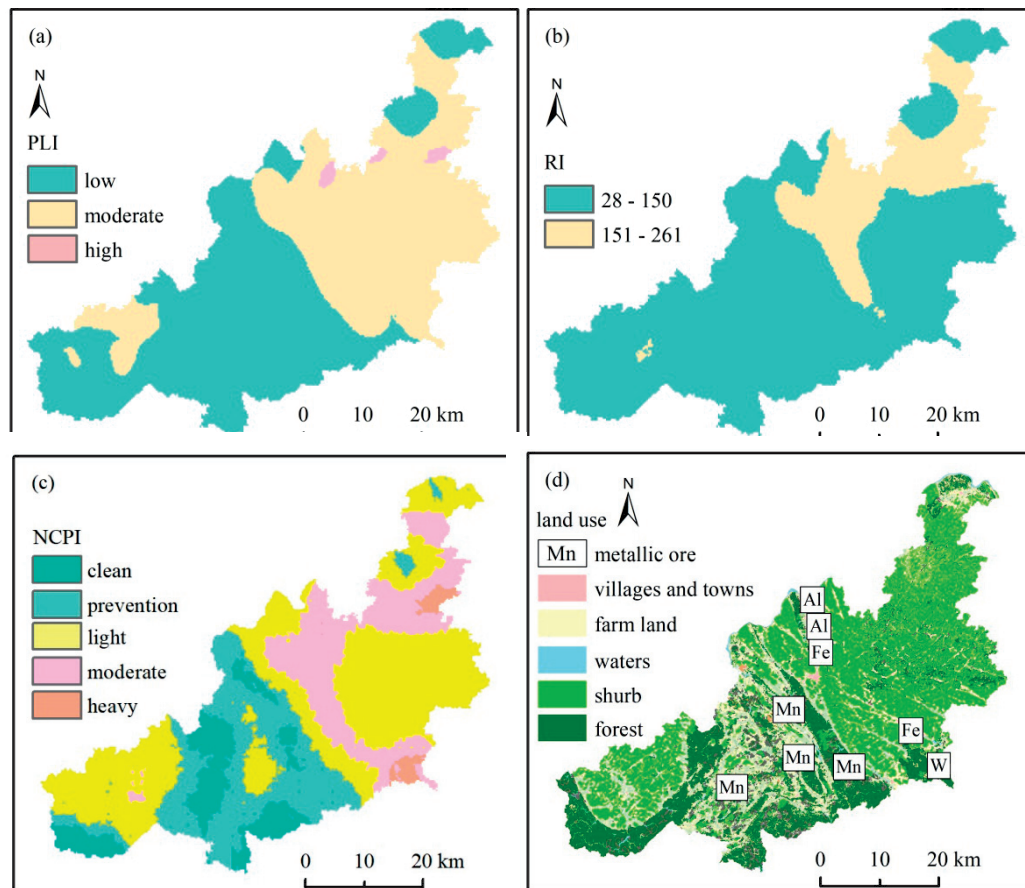


Fig. 4. Spatial distribution of PTE pollution risk assessment and land uses

oxide minerals through physicochemical mechanisms, involving adsorption, incorporation, and electron transfer [27-28]. Al is mainly influenced by geology background, and elevated in clay areas [29]. The soil Corg is not related to all PTEs, except that it has a low significant correlation coefficient of 0.156 with Pb, which is inconsistent with most previous research results [30]. Due to the diversity of types and sources of natural organic matter, and the complexity of their structure and properties, there is a certain degree of uncertainty in the interaction between organic matter and heavy metals [31].

Various degrees of soil pollution of PTE were reported in the karst regions [32-34]. The high content of heavy metals in carbonate rocks and the secondary enrichment in weathering form soils with a high background of heavy metals [11-32]. The concentration of PTE in lime soil is high, but in a relatively stable state under the background of calcium-rich geochemistry [35]. Cd in the karst areas of southwest China exceeded the standard rate of 95.83% in the previous study, but the water-soluble and exchangeable Cd concentration only accounted for 0.14% and 1.68%, respectively [36], and the Cd concentration in food crops does not exceed the edible safety standards [37]. However, 95% of rice grains harvested from limestone soil in Guangxi had a Cd concentration over the maximum permissible

concentration [38]. Therefore, risk assessment of heavy metal pollution in karst areas is needed to prevent harmful effects on human health.

Risk Assessment of PTE

According to GB 15618-2018, the concentration of Cd in the most soil sample was above the risk screening values, with a percentage of 75.74%, followed by Zn, As, Cr, Ni, Cu and Pb, with a percentage of 38.74%, 31.94%, 22.51%, 22.16%, 10.12%, and 0.52% of soil samples higher than the risk screening levels, respectively. The contamination levels of PTE in the soil were low or slightly moderate (Fig. 3). The P_i value was below 2 in almost all sampling sites (Fig. 3a). The average PLI value was 0.88 ± 0.52 , the maximum value of PLI reached 2.28. High PLI values were distributed in K, while low PLI values were distributed in the NK and KSC areas (Fig. 4a). The comparatively low and moderate PLI value proved that the soil underwent relatively slight-moderate contamination caused by high geological background.

The PEF_i was 10.00 ± 5.99 , 29.65 ± 31.82 , 1.98 ± 1.21 , 4.97 ± 1.59 , 39.79 ± 22.07 , 5.00 ± 3.29 , 5.00 ± 2.48 , and 0.99 ± 0.72 for As, Cd, Cr, Cu, Hg, Ni, Pb, and Zn, respectively (Fig. 3b). It showed that the soil was at a low pollution level, except for Cd and Hg in some

samples. The RI values ranged from 23.22 to 258.60, with an average value of 92.95 ± 58.95 (Fig. 3b). The spatial distribution of RI was the same as PLI, the high value was distributed in K, and the low value was distributed in NK and KSC (Fig. 4b).

The mean NCPI for soils was 1.47 at the light pollution level, and the contamination of Cd (mean $P_i > 1$) should be taken into account. The spatial distribution of NCPI was the same as that of lithology (Fig 4c). The light-moderate polluted areas were distributed in K, the prevention polluted areas were mainly distributed in KSC, and the clean areas were distributed in NK area (Fig. 4c). Consistency of light level in the NK and heavy polluted in KSC in some areas may be disturbed by the distribution of metallic ores and human activities (mining, agriculture, etc.) (Fig. 4d).

Mine drainage and the transportation of fine tailings led the average concentration of Cu, Zn, As, Cd and Pb in the surface soil of the farmland in the mining area 7 times higher than the corresponding background value, causing moderate to severe pollution [39]. Although mining activities in karst watersheds have been regulated for more than 30 years, the high geological background value of heavy metals in lime soil and the adverse ecological effects in the history of mining are still visible [40]. Land use also affects soil organic matter and aggregate particle size, and then immobilizes heavy metals through adsorption and so on [30]. Farmers have become heavily dependent on applying chemical fertilizers in poor soils, explaining the high Cd concentration in cultivated land [41]. The input of anthropogenic pollutants and fertilisers leads to the release of geologically caused Cd [42], which should focus on in future investigations and monitoring.

Conclusions

The average concentration of As, Cd, Cr, Cu, Hg, Ni, Pb and Zn in soils were 22.15 ± 13.27 , 2.35 ± 2.52 , 138.65 ± 85.06 , 39.89 ± 12.78 , 0.2 ± 0.11 , 60.43 ± 39.73 , 44.39 ± 22.03 and 197.9 ± 144.1 mg/kg, respectively. The soils were undergoing relatively low-moderate contamination except for the concentration of Cd exceeds the risk screening values of GB 15618-2018. Concerning the spatial pattern, most areas in K had high PTE concentrations, which were characterized by high concentration of Ca+Mg, Al, Fe, and high pH. Cd has a higher risk of contamination in the karst area. Pollution caused by PTE should be considered for farming in karst areas. Future studies should focus on speciation analysing and source apportionment of PTE in limestone soil.

Acknowledgments

This research was funded by Guangxi Science and Technology Programme (GUIKE AD21196001),

the Natural Science Foundation of Guangxi (2017GXNSFBFA198090), Guangxi Key Science and Technology Innovation Base on Karst Dynamics (KDL & Guangxi202209), Guilin Science and Technology Plan Project (2020010403), and the Research Program of the China Geological Survey (DD2016032403).

Conflict of Interest

The authors declare no conflict of interest.

References

- BASHIR S., HUSSAIN Q., AKMAL M., RIAZ M., HU H., IJAZ S.S., IQBAL M., ABRO S., MEHMOOD S., AHMAD M. Sugarcane bagasse-derived biochar reduces the cadmium and chromium bioavailability to mash bean and enhances the microbial activity in contaminated soil. *Journal of Soils and Sediments*. **18** (3), 874, **2018**.
- WAN M.X., HU W.Y., WANG H.F., TIAN K., HUANG B. Comprehensive assessment of heavy metal risk in soil-crop systems along the yangtze river in nanjing, southeast china. *Science of the Total Environment*. **780**, 146567, **2021**.
- TANG M.L., LU G.H., FAN B.L., XIANG W., BAO Z.Y. Bioaccumulation and risk assessment of heavy metals in soil-crop systems in liujiang karst area, southwestern china. *Environmental Science and Pollution Research*. **28** (8), 9657, **2021**.
- REHMAN A.U., NAZIR S., IRSHAD R., TAHIR K., UR REHMAN K., ISLAM R.U., WAHAB Z. Toxicity of heavy metals in plants and animals and their uptake by magnetic iron oxide nanoparticles. *Journal of Molecular Liquids*. **321**, 114455, **2021**.
- ENYA O., LIN C., QIN J. Heavy metal contamination status in soil-plant system in the upper mersey estuarine floodplain, northwest england. *Marine Pollution Bulletin*. **146**, 292, **2019**.
- WANG J.Y., CAI Y., YANG J., ZHAO X. W. Research trends and frontiers on source appointment of soil heavy metal: A scientometric review (2000-2020). *Environmental Science and Pollution Research*. **28** (38), 52764, **2021**.
- QU C., SHI W., GUO J., FANG B., WANG S., GIESY J. P., HOLM P. E. China's soil pollution control: Choices and challenges. *Environmental Science & Technology*. **50** (24), 13181, **2016**.
- BING H.J., QIU S.J., TIAN X., LI J., ZHU H., WU Y.H., ZHANG G. Trace metal contamination in soils from mountain regions across china: Spatial distribution, sources, and potential drivers. *Soil Ecology Letters*. **3** (3), 189, **2021**.
- JIANG Z.C., LIAN Y.Q., QIN X.Q. Rocky desertification in southwest china: Impacts, causes, and restoration. *Earth-Science Reviews*. **132** (0), 1, **2014**.
- WEN Y.B., LI W., YANG Z.F., ZHANG Q.Z., JI J.F. Enrichment and source identification of cd and other heavy metals in soils with high geochemical background in the karst region, southwestern china. *Chemosphere*. **245**, 125620, **2020**.
- YANG Q., YANG Z.F., FILIPPELLI G.M., JI J.F., JI W.B., LIU X., WANG L., YU T., WU T.S., ZHUO X.X., ZHANG Q.Z. Distribution and secondary enrichment of heavy

- metal elements in karstic soils with high geochemical background in guangxi, china. *Chemical Geology*. **567**, 120081, **2021**.
12. ZHANG Z., ZHANG Q., TU C., ZHANG J., LIN C., FANG H., WEN X. Effects on heavy metals in karst region soil and the enrichment characteristics of rice-rape rotation. *Polish Journal of Environmental Studies*. **28**(6), 4485, **2019**.
 13. ZINN Y.L., FARIA J.A.D., ARAUJO M.A.D., SKORUPA A.L.A. Soil parent material is the main control on heavy metal concentrations in tropical highlands of brazil. *Catena*. **185**, 104319, **2020**.
 14. KONG J., GUO Q.J., WEI R.F., STRAUSS H., ZHU G.X., LI S.L., SONG Z.L., CHEN T.B., SONG B., ZHOU T., ZHENG G.D. Contamination of heavy metals and isotopic tracing of pb in surface and profile soils in a polluted farmland from a typical karst area in southern china. *Science of the Total Environment*. **637-638**, 1035, **2018**.
 15. LIU N.T., LIU H.Y., WU P., MENG W., LI X.X., CHEN X. Distribution characteristics and potential pollution assessment of heavy metals (Cd, Pb, Zn) in reservoir sediments from a historical artisanal zinc smelting area in southwest china. *Environmental Science and Pollution Research*. **2021**.
 16. WU H.W., LIU Q.Y., MA J., LIU L.L., QU Y.J., GONG Y.W., YANG S.H., LUO T. Heavy metal(loids) in typical chinese tobacco-growing soils: Concentrations, influence factors and potential health risks. *Chemosphere*. **245**, 125591, **2020**.
 17. ZHANG C., ZOU X., YANG H., LIANG J., ZHU T. Bioaccumulation and risk assessment of potentially toxic elements in soil-rice system in karst area, southwest china. *Frontiers in Environmental Science*. **10**, 866427, **2022**.
 18. MLRPRC M. O. L. A. R. O. T. P. S. R. O. C. Specification of land quality geochemical assessment. Geological Publishing House, **2016**.
 19. TOMLINSON D.L., WILSON J.G., HARRIS C.R., JEFFREY D.W. Problems in the assessment of heavy-metal levels in estuaries and the formation of a pollution index. *Helgolinder Meeresuntersuchungen*. **33** (1), 566, **1980**.
 20. HU B.F., JIA X.L., HU J., XU D.Y., XIA F., LI Y. Assessment of heavy metal pollution and health risks in the soil-plant-human system in the yangtze river delta, china. *International Journal of Environmental Research and Public Health*. **14** (9), 1042, **2017**.
 21. HAKANSON L. An ecological risk index for aquatic pollution control. A sedimentological approach. *Water Research*. **14** (8), 975, **1980**.
 22. GU X., XU L., WANG Z.X., MING X., DANG P., OUYANG W., LIN C.Y., LIU X.T., HE M.C., WANG B.D. Assessment of cadmium pollution and subsequent ecological and health risks in jiaozhou bay of the yellow sea. *Science of the Total Environment*. **774**, 145016, **2021**.
 23. DANG P., GU X., LIN C.Y., XIN M., ZHANG H., OUYANG W., LIU X.T., HE M.C., WANG B.D. Distribution, sources, and ecological risks of potentially toxic elements in the laizhou bay, bohai sea: Under the long-term impact of the yellow river input. *Journal of Hazardous Materials*. **413**, 125429, **2021**.
 24. HOU Q.Y., YANG Z.F., YU T., XIA X.Q., CHENG H. X., ZHOU G.H. Soil geochemical parameters in china. Beijing, Geological Publishing House, 2654, **2020**.
 25. HU B.Q., JIANG S.F., LIAO C.M., YAN Z.Q. Tupu analysis on driving mechanism of guangxi karst rocky desertification based on 3s techniques. *Journal of Mountain Science*. **24** (2), 234, **2006**.
 26. JI W.B., YANG Z.F., YU T., YANG Q., WEN Y.B., WU T.S. Potential ecological risk assessment of heavy metals in the fe-mn nodules in the karst area of guangxi, southwest china. *Bulletin of Environmental Contamination and Toxicology*. **106** (1), 51, **2021**.
 27. FRIERDICH A.J., CATALANO J.G. Distribution and speciation of trace elements in iron and manganese oxide cave deposits. *Geochimica et Cosmochimica Acta*. **91**, 240, **2012**.
 28. ZHOU Q.W., LIAO B.H., LIN L.N., SONG Z.G., KHAN Z.H., LEI M. Characteristic of adsorption cadmium of red soil amended with a ferromanganese oxide-biochar composite. *Environmental Science and Pollution Research*. **26** (5), 5155, **2019**.
 29. MENG Y.T., CAVE M., ZHANG C.S. Identifying geogenic and anthropogenic controls on different spatial distribution patterns of aluminium, calcium and lead in urban topsoil of greater london authority area. *Chemosphere*. **238**, 124541, **2020**.
 30. ZHANG Q., HAN G.L., LIU M., LIANG T. Spatial distribution and controlling factors of heavy metals in soils from pudong karst critical zone observatory, southwest china. *Environmental Earth Sciences*. **78** (9), 279, **2019**.
 31. LI L., WANG Z.Y., LIN D.H., WU F.C. Advances in analytical methods for investigating the interaction between natural organic matters and heavy metals. *Research of Environmental Sciences*. **2**, 182, **2015**.
 32. MA H.H., PENG M., LIU F., GUO F., CHENG H.X. Bioavailability, translocation, and accumulation characteristic of heavy metals in a soil-crop system from a typical carbonate rock area in guangxi, china. *Environmental Science*. **41** (1), 449, **2020**.
 33. ZHANG C.L., LI Z.Y., YANG W.W., PAN L.P., GU M.H., DOKYOUNG L. Assessment of metals pollution on agricultural soil surrounding a lead-zinc mining area in the karst region of guangxi, china. *Bulletin of Environmental Contamination and Toxicology*. **90**, 736, **2013**.
 34. LIU P.F., WU Z.Q., LUO X.R., WEN M.L., HUANG L.L., CHEN B., ZHENG C.J., ZHU C., LIANG R. Pollution assessment and source analysis of heavy metals in acidic farmland of the karst region in southern china – a case study of quanzhou county. *Applied Geochemistry*. **123**, 104764, **2020**.
 35. DENG Q.C., WEI Y.P., YIN J., CHEN L.J., PENG C., WANG X.F., ZHU K.X. Ecological risk of human health in sediments in a karstic river basin with high longevity population. *Environmental Pollution*. **265**, 114418, **2020**.
 36. ZHU D.N., ZOU S.Z., ZHOU C.S., LI L.J., LU H.P. Cd²⁺ adsorption characteristics of typical soils in karst areas. *Carsologica Sinica*. **34** (4), 402, **2015**.
 37. TIAN H.Y., ZHANG C., QI S.H., KONG X.S., YUE X.F. Concentration and spatial distribution of potentially toxic elements in surface soil of a peak-cluster depression, babao town, yunnan province, china. *International Journal of Environmental Research and Public Health*. **18** (6), 3122, **2021**.
 38. LI D.Q., LI W.Y., LU Q., LI Y.T., LI N., XU H.J., REN Z.L., ZHANG Y.L., WANG J.J. Cadmium bioavailability well assessed by dgt and factors influencing cadmium accumulation in rice grains from paddy soils of three parent materials. *Journal of Soils and Sediments*. **18** (7), 2552, **2018**.
 39. SUN Z.H., XIE X.D., WANG P., HU Y.N., CHENG H. F. Heavy metal pollution caused by small-scale metal ore

- mining activities: A case study from a polymetallic mine in south china. *Science of the Total Environment*. **639**, 217, **2018**.
40. WU W.H., QU S.Y., NEL W., JI J.F. The impact of natural weathering and mining on heavy metal accumulation in the karst areas of the pearl river basin, china. *Science of the Total Environment*. **734**, 139480, **2020**.
41. CHEN X.X., LIU Y.M., ZHAO Q.Y., CAO W.Q., CHEN X.P., ZOU C.Q. Health risk assessment associated with heavy metal accumulation in wheat after long-term phosphorus fertilizer application. *Environmental Pollution*. **262**, 114348, **2020**.
42. KUBIER A., WILKIN R.T., PICHLER T. Cadmium in soils and groundwater: A review. *Applied Geochemistry*. **108**, 104388, **2019**.